Improved idler beam quality via simultaneous parametric oscillation and signal-to-idler conversion

Shani Sharabi,* Gil Porat, and Ady Arie

Department of Physical Electronics, Faculty of Engineering, Tel-Aviv University, Tel-Aviv 69978, Israel
**Corresponding author: shanis@post.tau.ac.il*

Received January 2, 2014; revised February 28, 2014; accepted March 4, 2014;
posted March 4, 2014 (Doc. ID 203970); published March 31, 2014

We report on an improvement of idler beam quality in a singly resonant optical parametric oscillator (OPO), where the resonant signal is converted to the idler via an additional difference frequency generation (DFG) process. The two processes are phase matched simultaneously by a quasi-periodically poled nonlinear crystal. Whereas back-conversion of the signal and idler to the pump frequency distorts the idler beam in a standard OPO, in a quasi-periodic OPO the DFG process reduces the signal intensity, leading to suppression of back-conversion and, hence, improvement in idler beam quality. Indeed, the experimental results show under the same pump power a significant improvement in idler beam quality for the quasi-periodic OPO ($1 \le M^2 \le 2.1$) as compared with the standard OPO ($3.2 \le M^2 \le 5.3$). © 2014 Optical Society of America

OCIS codes: (190.0190) Nonlinear optics; (190.4970) Parametric oscillators and amplifiers; (190.4223) Nonlinear wave mixing.
http://dx.doi.org/10.1364/OL.39.002152

In a singly resonant optical parametric oscillator (OPO), the idler wave is not constrained by the cavity mirrors and tends to suffer from poor beam quality. The main mechanism that deteriorates the beam quality is back-conversion of the signal and idler waves to the pump frequency [1,2]. Owing to its nonlinearity, the back-conversion process is usually most pronounced at the highest intensities, which are obtained at the central part of the beam for Gaussian-like beams. Consequently, back-conversion results in an idler beam with reduced intensity at the central part of the beam, which leads to a much larger divergence with respect to an ideal Gaussian beam.

Several works were focused on improving the beam quality of OPOs. High beam quality was achieved by using special collinear phase matching [3], special non-collinear phase matching [4], image rotation resonators [3,5,6] and unstable resonators combined with a long pump pulse duration [7].

Here we report on a new scheme for improving the idler beam quality, which is based on an OPO that supports an additional nonlinear difference frequency generation (DFG) process that converts the signal to the idler. The original motivation for studying this scheme is the improvement in pump-to-idler conversion efficiency: whereas a standard OPO is fundamentally limited by quantum efficiency (ω_i/ω_p, which is only 25% for conversion of a 1 μm pump to a 4 μm idler), the OPO–DFG scheme facilitates the conversion of signal photons into additional idler photons and, therefore, improves the overall pump-to-idler conversion efficiency. This scheme was first proposed using two independent periodically poled nonlinear crystals in the same cavity [8–10]. It was extended further by using a single crystal, with cascaded gratings, for both processes [10–12]. Recently, this concept was realized in a single nonlinear crystal that simultaneously phase-matched the OPO and DFG processes [13–15]. This was achieved by quasi-periodic modulation of the nonlinear coefficient [16]. Here we show a surprising effect—in addition to the expected improvement in efficiency, the quasi-periodic OPO also provides an idler wave with better beam quality. This improvement in beam quality was reported recently for a dual-grating OPO [12], having different sections in the crystal for parametric oscillation and signal-to-idler conversion. Here we show improvement in beam quality for a quasi-periodic OPO, in which both nonlinear processes occur simultaneously. In addition, we show by numerical simulation that the origin of this effect is the suppression of the back-conversion process.

Quasi-periodic modulation of the nonlinear coefficient is a method to simultaneously phase match several processes [16,17]. In our case, we would like to phase match two processes, i.e., the OPO process and the DFG process. For designing the quasi-periodic structure, we used the dual-grid method [16]. The design parameters used here are the same as in [11], except that thermal expansion of the ferroelectric domains [18] was precompensated. By applying a one-dimensional version of the dual-grid method, we obtained a quasi-periodic sequence of two building blocks, labeled A and B, with lengths of 16.25 and 14.28 μm, respectively. This one-dimensional quasi-crystal has the desired wave vectors in its reciprocal lattice, with a Fourier coefficient of ~0.4 for each of the two processes [13]. A nonlinear quasi-periodic crystal is obtained by modulating the nonlinear coefficient in the A and B blocks to be positive and negative, respectively.

We have prepared two parallel gratings on the same crystal: one periodic with a period of 28.8 μm and the other quasi-periodic, as outlined above. The nonlinear coefficient was modulated by electric field poling of 5% MgO-doped congruently grown $LiNbO_3$ (MgCLN). The desired patterns were achieved by applying an electric field through patterned electrodes on the crystal surface [19]. The crystal was 40 mm long, and its input and output surfaces were antireflection (AR)-coated for the pump, signal, and idler waves. The temperature for optimum conversion efficiency was designed to be 125°C.

The output beams of the two OPOs were measured using the experimental setup shown in Fig. 1. The pump source, a 5.5 ns full width at half-maximum (FWHM) Nd:YAG laser with a repetition rate of 10 kHz, lasing at

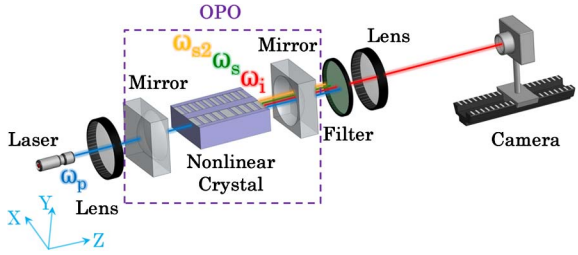

Fig. 1. Experimental setup.

$\lambda_p \sim 1064.5$ nm, was focused with a waist of ~130 μm at the center of the 40 mm crystal that was placed in a singly resonant 55 mm long linear cavity. The cavity was made of two mirrors with a 50 mm radius of curvature. The input mirror was AR-coated for the pump and idler, and had ~99% reflection for the signal. The output mirror was AR-coated for the idler, and had ~89% and ~15% reflection for the signal and pump, respectively. The nonlinear crystal was housed in a temperature controlled oven at a temperature of 118.2°C where optimum conversion efficiency was measured. We assume that the difference between the experimental and theoretical temperatures is caused by inaccuracies in the Sellmeier coefficients [20] and in determining the crystal temperature. Spectral filters were placed after the OPO in order to measure each of the different beams separately. In order to measure the beam profile and power, we also used a 15 cm lens, a Pyrocam IR camera (Spiricon), a power meter, and an optical spectrum analyzer.

In the experiment, the signal and idler wavelengths for the two gratings were $\lambda_s \sim 1462.4$ nm and $\lambda_i \sim 3910.9$ nm, respectively. The additional wavelength generated by the DFG process was 2336.3 nm, as calculated from energy conservation. Figure 2(a) shows the measured power of the OPO idler radiation. The threshold of the quasi-periodic grating (311 mW) is higher than the threshold of the periodic grating (119 mW). This is due to the requirement that the quasi-periodic structure will quasi-phase-match the additional DFG process. However, whereas the efficiency slope of the periodic grating is 7.8%, the quasi-periodic grating's efficiency slope is almost twice higher (14.5%). Consequently, at pump powers above 541 mW, the quasi-periodic OPO idler power was higher, reaching 171.9 mW as compared with 108.3 mW for the periodic grating. These values were obtained for an estimated pump coupling efficiency of ~70%. The experimental spatial intensity profiles of the OPO idler radiation for some representative input powers are also illustrated in Fig. 2(b). These beam profiles were measured at a distance of 12.2 cm after an external lens of 15 cm. This location is ~24.3 cm before the waist location of the idler beam. It can be seen that for the periodic grating (top row) the idler beam size increases as the pump power increases, whereas beam size is only weakly affected by pump power for the quasi-periodic grating (bottom row). Moreover, comparing the results obtained at the *same* pump power in the three different cases shown here indicates that the periodic structure yields a larger beam size with respect to the quasi-periodic structure.

We have simulated [21] the two OPOs using a split-step beam propagation program, which used the parameters

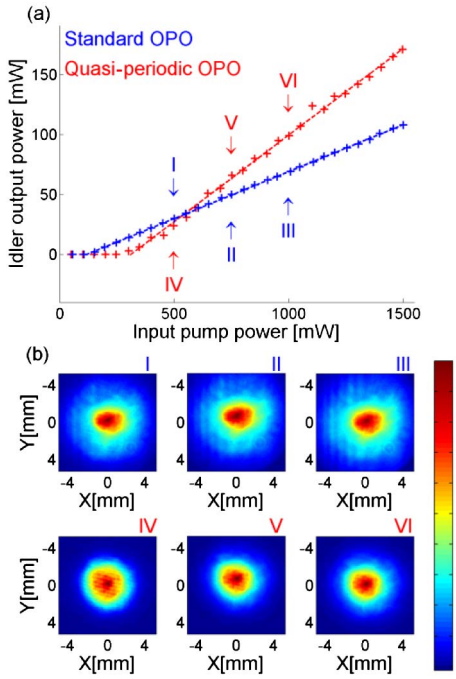

Fig. 2. (a) Measured results for the idler output power of standard (blue) and quasi-periodic (red) OPOs as a function of input pump power. The solid lines are linear fits to the measured results. (b) Experimental spatial intensity profiles of periodic (top row) and quasi-periodic (bottom row) OPO idler radiation.

of the experimental setup. We used the published value of the nonlinear coefficients of MgCLN [22,23] and corrected them for the different interacting wavelengths using Miller's rule [22] ($d_{\mathrm{OPO}} = 20.025$ pm/V, $d_{\mathrm{DFG}} = 19.144$ pm/V). For perfect coupling, the quasi-periodic OPO will have a threshold of 258 mW and a slope efficiency of 20.3%, whereas the standard OPO will have a threshold of 85 mW and a slope efficiency of 12.0%. Taking into account the coupling efficiency of the pump, the thresholds for the periodic and quasi-periodic OPOs are 121 and 369 mW, respectively, which is reasonably close to the measured values. We have then used this simulation to calculate the output idler pump power and the beam quality factor M^2 [2,21] as a function of time for a 5.5 ns FWHM Gaussian pump pulse energy of ~53 μJ (corresponding to 500 mW average power), as shown in Fig. 3. This pump power was selected to illustrate the effect because the idler powers of the standard and quasi-periodic OPOs are almost identical to this pump power. For an ideal beam with a Gaussian spatial intensity distribution and a uniform phase front at the waist location, the value of the beam quality factor, M^2, is 1, along any transverse direction. However, for other beams this factor increases, thereby representing faster divergence.

Back-conversion of the idler wave is shown clearly in Fig. 3(a), leading to sharp decreases of power shortly after the threshold is reached. This is accompanied by a distortion of the intensity profile (two representative cases of the intensity profile at the OPO exit plane are shown in the insets) and an increase in the M^2. In contrary to that, the back-conversion process in the quasi-periodic OPO is suppressed, and, therefore, idler power

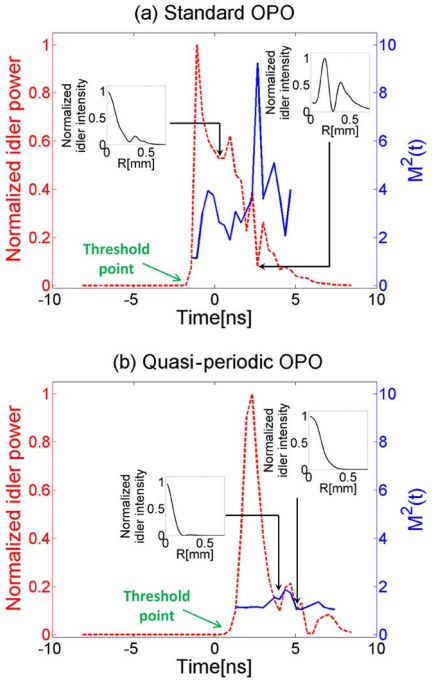

Fig. 3. Simulations of the temporal behavior of both (a) standard and (b) quasi-periodic OPOs with ~53 μJ pump pulse energy (corresponding to 500 mW average power): normalized power profile (red) and beam quality factor M^2 (blue) as a function of time. Inset: spatial intensity profiles at a specific time.

is rather smooth shortly after the threshold and exhibits only minor ripples, as shown in Fig. 3(b). As can be seen in Fig. 3(a), M^2 is highest when dips in the temporal profile occur, i.e., when the idler wave back-converts to the pump wave. However, in the quasi-periodic case the beam quality is nearly constant and M^2 is much lower than that in the periodic case [Fig. 3(b)]. This confirms our assumption on the effect of back-conversion on beam quality. We note that the same improvement in beam quality was observed in simulations for different pump levels, for longer pump pulses, and even in the case in which parametric amplification and signal-to-idler conversion are performed separately in cascaded periodic crystals [9].

The simulation enables us to examine the evolution of idler power and beam quality as a function of time, and to demonstrate explicitly the effect of back-conversion. In the experiment, we measure the time-integrated result for the entire pulse, but obviously, the improvement in the beam quality for the quasi-periodic OPO is also shown here.

Figure 4 shows the measurement of beam width at a fixed pump power of 1000 mW for the two OPOs. The idler output intensity profiles were recorded at various positions along the beam propagation axis for both sides of the waist, which was formed by a 150 mm focusing lens. For each of the two perpendicular axes, beam width is defined as twice the square root of the second moment of intensity along each one of the two transverse coordinates (x or y) [24]. The value of M^2 was extracted by fitting the measured widths. For x axis, beam width W_x is related to beam quality factor M_x^2 by

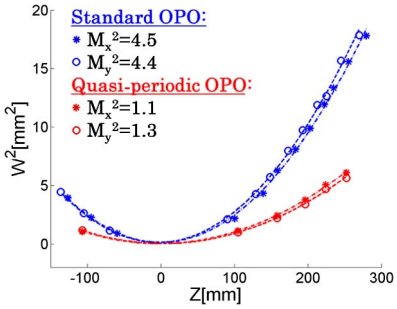

Fig. 4. Comparison between standard (blue) and quasi-periodic (red) measured divergence: square of beam width as a function of the distance from the waist in the two orthogonal axes x (solid stars) and y (open circles). The dashed curves are fits to the experimental values indicated by the markers. Input pump power was 1000 mW.

$$W_x^2(z) = W_{0x}^2 + M_x^4 \cdot \left(\frac{\lambda}{\pi W_{0x}}\right)(z - z_{0x})^2, \qquad (1)$$

where z is the beam propagation direction, W_{0x} is the x axis Gaussian beam waist positioned at z_{0x}, and λ is the wavelength. The same relations hold for any transverse direction, e.g., the vertical y axis.

As can be seen, the divergence of the idler wave, as well as the corresponding M^2 values, in the case of a standard OPO are much larger than those obtained with a quasi-periodic OPO.

Figure 5(a) depicts the average (between the two orthogonal axes x and y) of the measured M^2 values as a function of input pump power. We found that the idler wave of the quasi-periodic OPO was characterized by M^2 values that were consistently lower by a factor of ~3 compared with those of the standard OPO. Furthermore, for both OPOs, a degradation of beam quality was observed as the input pump power increased. For comparison, Fig. 5(b) illustrates numerical simulation results [2,21] with similar behavior. Here, we calculated the time-averaged M^2 over the entire pulse and obtained an average ratio of 2.3 between the M^2 values in the periodic and quasi-periodic cases. The slight difference between the experimental and simulated results can be attributed to additional ignored parasitic processes in the simulation, e.g., second harmonic of the pump; to multi-longitudinal-mode operation, neglected in the simulation; to thermal gradients in the crystal, which locally shift the

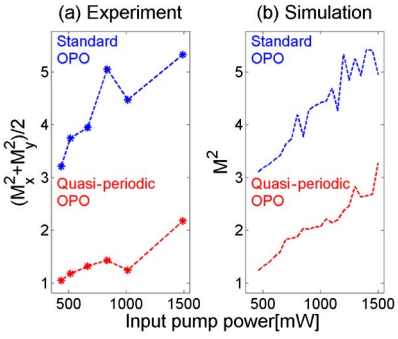

Fig. 5. Comparison between standard and quasi-periodic OPO idler beam quality as a function of input pump power. (a) Experiment and (b) simulation.

phase matched wavelength; and deviations of the actual poling pattern from the theoretical design. Quasi-periodic OPO with high idler power was demonstrated recently [15]. Our numerical simulation shows that beam quality improvement is also expected at multiple watt levels.

The M^2 values of the signal beam were also measured. The two OPOs exhibited nearly the same values, growing from 1.7 to 4 as pump input power increased from 430 to 1500 mW. Since the signal beam is resonant in the cavity, its shape is predominantly controlled by the geometry of the cavity and pump power, which together determine the number of oscillating transverse modes. As pump power increases, so does the number of oscillating transverse modes, and, hence, the degradation in the signal beam quality.

In conclusion, we have demonstrated experimentally and theoretically that using a quasi-periodic OPO instead of the standard OPO can significantly improve the quality of the idler beam: the quasi-periodic OPO beam quality parameter was smaller by a factor of ~3. Furthermore, the proposed OPO also exhibited a higher conversion efficiency [13].

Whereas here a single quasi-periodically poled crystal was used to phase match the two nonlinear processes, we expect that improvement in the beam quality of the idler can also be obtained in OPOs in which the two processes are phase-matched separately [12]. Furthermore, other methods to suppress back-conversion, e.g., by shaping the pump pulse [25], are also expected to improve the idler beam quality.

This work was supported by the Israel Science Foundation and the Office of Chief Scientist of the Ministry of Economy.

References

1. R. Urschel, A. Borsutzky, and R. Wallenstein, Appl. Phys. B **70**, 203 (2000).
2. A. V. Smith, W. J. Alford, T. D. Raymond, and M. S. Bowers, J. Opt. Soc. Am. B **12**, 2253 (1995).
3. G. Anstett, G. Göritz, D. Kabs, R. Urschel, R. Wallenstein, and A. Borsutzky, Appl. Phys. B **72**, 583 (2001).
4. C. D. Nabors and G. Frangineas, Adv. Solid-State Lasers **10**, 90 (1997).
5. D. J. Armstrong and A. V. Smith, Opt. Lett. **27**, 40 (2002).
6. A. V. Smith and M. S. Bowers, J. Opt. Soc. Am. B **18**, 706 (2001).
7. S. Pearl, Y. Ehrlich, S. Fastig, and S. Rosenwaks, Appl. Opt. **42**, 1048 (2003).
8. K. Koch, G. T. Moore, and E. C. Cheungy, J. Opt. Soc. Am. B **12**, 2268 (1995).
9. M. E. Dearborn, K. Koch, G. T. Moore, and J. C. Diels, Opt. Lett. **23**, 759 (1998).
10. W. Zhang, Opt. Commun. **274**, 451 (2007).
11. K. A. Tillman, D. T. Reid, D. Artigas, and T. Y. Jiang, J. Opt. Soc. Am. B **21**, 1551 (2004).
12. A. Godard, M. Raybaut, M. Lefebvre, A.-M. Michel, and M. Péalat, Appl. Phys. B **109**, 567 (2012).
13. G. Porat, O. Gayer, and A. Arie, Opt. Lett. **35**, 1401 (2010).
14. O. P. Naraniya, M. R. Shenoy, and K. Thyagarajan, Appl. Opt. **51**, 1312 (2012).
15. T. Chen, B. Wu, P. Jiang, D. Yang, and Y. Shen, IEEE Photon. Technol. Lett. **25**, 2000 (2013).
16. R. Lifshitz, A. Arie, and A. Bahabad, Phys. Rev. Lett. **95**, 133901 (2005).
17. S. Zhu, Science **278**, 843 (1997).
18. Y. S. Kim, J. Appl. Phys. **40**, 4637 (1969).
19. M. Yamada, N. Nada, M. Saitoh, and K. Watanabe, Appl. Phys. Lett. **62**, 435 (1993).
20. O. Gayer, Z. Sacks, E. Galun, and A. Arie, Appl. Phys. B **91**, 343 (2008).
21. A. V. Smith, R. J. Gehr, and M. S. Bowers, J. Opt. Soc. Am. B **16**, 609 (1999).
22. R. C. Miller, Appl. Phys. Lett. **5**, 17 (1964).
23. I. Shoji, T. Kondo, A. Kitamoto, M. Shirane, and R. Ito, J. Opt. Soc. Am. B **14**, 2268 (1997).
24. A. E. Siegman, in *DPSS (Diode Pumped Solid State) Lasers: Applications and Issues*, M. Dowley, ed., Vol. **17** of OSA Trends in Optics and Photonics (Optical Society of America, 1998), paper MQ1.
25. Z. Sacks, O. Gayer, E. Tal, and A. Arie, Opt. Express **18**, 12669 (2010).